Journal of Materials Chemistry

Cite this: *J. Mater. Chem.*, 2011, **21**, 18768

www.rsc.org/materials

PAPER

Flow reactor synthesis of CdSe, CdS, CdSe/CdS and CdSeS nanoparticles from single molecular precursor(s)

Ahmed Lutfi Abdelhady,[a] Mohammad Afzaal,[ab] Mohammad Azad Malik[a] and Paul O'Brien*[a]

Received 27th July 2011, Accepted 28th September 2011
DOI: 10.1039/c1jm13590b

$[Cd(S_2CNMe^nHex)_2]$ and $[Cd(Se_2P^iPr_2)_2]$ were used as single source precursors (SSPs) in oleylamine for the synthesis of CdS, CdSe, CdSe/CdS, and CdSeS nanoparticles in a microcapillary reactor. The influence of the different reaction parameters (precursor concentration, growth temperature and residence time) on the size and the optical properties of the nanoparticles were studied. Transmission electron microscopy (TEM) showed that CdS nanoparticles were in the range of 5.0 to 8.0 nm whereas the CdSe nanoparticles were small (*ca.* 2 nm) with blue luminescence irrespective of the growth temperature, concentration or residence time. The CdSe/CdS core/shell and the CdSeS alloys were bluish green or green luminescent depending on their size.

Introduction

In recent years, continuous flow synthesis in microreactors has emerged as a novel and potentially good route for nanoparticles synthesis.[1] The main potential advantages of this method are the rapid and continuous screening of reaction parameters, efficient mixing of reagents providing a homogeneous reaction environment, varying the composition of the reaction mixture by varying the injection rates, online analysis and continuous production. The synthesis of cadmium selenide (CdSe) nanoparticles in microreactors has been reported by different research groups. Alivisatos *et al.*[2] prepared CdSe nanoparticles by injecting a mixture of Se/$CdMe_2$/tributylphosphine, dodecylamine, trioctylphosphine (TOP) and octadecene (ODE) into a chip using a syringe pump. Other research groups prepared CdSe nanoparticles in microfluidic reactors using a mixture of cadmium acetate, TOPSe and trioctylphosphine oxide (TOPO).[3–5] Bawendi *et al.*[6] avoided the use of $CdMe_2$ and TOPO in the synthesis of CdSe nanoparticles; $CdMe_2$ causes gas evolution and TOPO can decompose and block the reactor. Instead, they used cadmium hydroxide in a mixture of oleic acid, squalane and oleylamine as a Cd precursor and TOPSe. These precursors were injected in two separate flows. Mathies *et al.*[7] reported the synthesis of CdSe nanoparticles in nanolitre-volume droplets in a microfabricated reactor to overcome the possibility of particles deposition on the channel walls. A gas–liquid segmented flow instead of the liquid–liquid was also investigated.[8] In the continuing search for an optimal microreactor, a small tube furnace with distributed temperature zone was used to separate the nucleation and growth steps for the synthesis of more monodispersed CdSe nanoparticles.[9] A serpentine microchannel was also used for the synthesis of CdSe nanoparticles as it offers homogeneous residence time and monomer concentration at fast flow rates.[10] Recently, a combinatorial synthesis system composed of several microreactors and an online detector was reported for the rapid synthesis of CdSe nanoparticles.[11]

Cadmium sulfide (CdS) nanoparticles were also synthesised using the continuous flow method. In 1992, Fischer and Giersig[12] introduced a fast flow technique in which two solutions containing Cd^{2+} and SH^- ions were mixed forming 1.3 nm CdS nanoparticles. de Mello *et al.*[13] reported the synthesis of CdS nanoparticles *via* microfluidic routes using aqueous solutions of cadmium nitrate and sodium sulfide mixed with an equal amount of sodium polyphosphate. In a different process, CdS nanoparticles with different sizes were produced at a constant temperature and residence time by varying the feed ratio of the cadmium and sulfur precursors.[14]

Surface passivation is critical for the photoluminescence (PL) and quantum yield (QY) of the nanoparticles.[15] Methods for coating a semiconductor nanoparticle with another semiconductor forming a core/shell material are well developed and different core/shell structures have been reported both in conventional batch methods and continuous flow methods. In continuous flow synthesis, CdSe/ZnS core/shell is the most explored material. Maeda *et al.*[16] prepared CdSe/ZnS core/shell nanoparticles in a multi-step continuous system composed of a CdSe synthesis section, followed by mixing of $[Zn(S_2CNEt_2)_2]$ as a shelling material. QYs greater than 50% are reported for the CdSe/ZnS nanoparticles.[17] Separate injection of equal volumes of CdSe nanoparticles and $[Zn(S_2CNEt_2)_2]$ into polytetrafluoroethylene microcapillary tubes produced green luminescent CdSe/ZnS core/shell nanoparticles.[18] Recently, full colour

[a]*The School of Chemistry and The School of Materials, The University of Manchester, Manchester, UK. E-mail: paul.obrien@manchester.ac.uk; Fax: +44 161 275 4598; Tel: +44 161 275 4653*
[b]*Present address: Center of Research Excellence in Renewable Energy, King Fahd University of Petroleum and Minerals, P.O. Box 1292, Dhahran, 31261, Saudi Arabia*

emitting CdS/ZnS and CdSe/ZnS core/shell nanoparticles were prepared in a microreactor using mixtures of cadmium oxide in oleic acid, oleylamine (OLA) and ODE, elemental sulfur in OLA and ODE, elemental selenium in TOP, OLA and ODE as the cadmium, sulfur and selenium precursors, respectively, and finally $[Zn(S_2CNEt_2)_2]$ in TOP, OLA and ODE as the raw material for the ZnS shell.[14]

Another heterogeneous nanostructure is the alloyed CdSeS nanoparticles. Controlling the composition of the different elements in the alloy provides a good mean of tuning the band gap of the nanoparticles. A general route for the synthesis of the CdSeS nanoparticles is the injection of a mixture of the selenium and sulfur precursors into a hot high boiling coordinating solvent containing the cadmium precursor.[19,20] $CdSe_xS_y$ was synthesised by Al-Salim *et al.*[21] in different organic solvents with different coordinating properties. In addition, a noninjection one-pot method was reported by Yu *et al.*[22] for the synthesis of homogeneously alloyed CdSeS nanoparticles.

To the best of our knowledge there are no reports on the use of SSPs for the synthesis of CdSe, CdS, CdSe/CdS core/shell, or CdSeS alloy nanoparticles in microreactors. In this paper, $[Cd(S_2CNMe^nHex)_2]$ and $[Cd(Se_2P^iPr_2)_2]$ were used as SSPs for CdS and CdSe, respectively. The synthesis of these materials was carried out in a microcapillary reactor. OLA was chosen as a capping agent because of its good ability, as a primary amine, to achieve high PL.[23,24] Furthermore, OLA has low melting point, *i.e.* liquid at room temperature, which lowers the probability of the microreactor channels getting clogged. CdS is considered to be a good shelling material for CdSe; it has a larger band gap compared to that of CdSe and the lattice mismatch between CdSe (core) and CdS (shell) is only 3.9%.[25]

Experimental

All reagents were purchased from Sigma-Aldrich chemical company and used as received. Solvents were distilled prior to use.

Experimental setup

A fused silica microcapillary tube with an inner diameter of 150 μm and an outer diameter of 360 μm was used as a microreactor. 40 cm of the microcapillary tube was immersed in an oil bath for heating purpose. The reaction solution was loaded to a gastight syringe that was connected to a pump (PHD 2000 Infusion) in order to inject the solution through the capillary tube, as shown in Fig. 1.

Synthesis of precursors

The preparation of $[Cd(Se_2P^iPr_2)_2]$[26] and $[Cd(S_2CNMe^nHex)_2]$[27] were carried out according to literature methods.

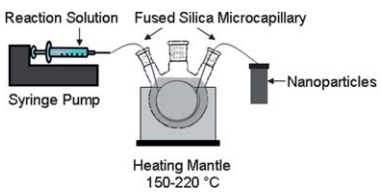

Fig. 1 Illustration of the experimental setup using the microcapillary reactor.

Synthesis of CdSe nanoparticles from $[Cd(Se_2P^iPr_2)_2]$

Effect of concentration. A series of different precursor concentrations were prepared by dissolving $[Cd(Se_2P^iPr_2)_2]$ in 2 mL TOP. The concentrations were as follows: 5×10^{-3} M, 1×10^{-2} M and 2×10^{-2} M. Then 8 mL of OLA was added to each solution. The mixtures were loaded into a syringe, and injected into the fused silica microcapillary tube. The microcapillary tube was pre-heated at 200 °C and the residence time was kept constant at 8.4 s using a flow rate of 50 μL min^{-1}.

Effect of temperature. Three different temperatures (180 °C, 200 °C and 220 °C) were studied. The concentration of $[Cd(Se_2P^iPr_2)_2]$ used in this study was 2×10^{-2} M and the flow rate was kept at 50 μL min^{-1} (residence time = 8.4 s).

Effect of residence time. In order to study the effect of the residence time, the concentration of $[Cd(Se_2P^iPr_2)_2]$ and the temperature were kept constant at 2×10^{-2} M and 200 °C, respectively. Residence times were studied between 4.2 s and 16.8 s.

Synthesis of CdS nanoparticles from $[Cd(S_2CNMe^nHex)_2]$

Effect of concentration. Three different concentrations were prepared: 0.5 mM, 1 mM and 2 mM by adding $[Cd(S_2CNMe^nHex)_2]$ (2.5 mg, 5×10^{-3} mmol), (5 mg, 1×10^{-2} mmol) and (10 mg, 2×10^{-2} mmol) into OLA (10 mL), respectively. The mixtures were loaded into a syringe and injected into the fused silica microcapillary tube. The microcapillary tube was pre-heated at 200 °C and the residence time was kept constant at 8.4 s using a flow rate of 50 μL min^{-1}.

Effect of temperature. Three different temperatures were studied: 160 °C, 180 °C and 200 °C. The concentration used in this study was 2 mM and the flow rate was 50 μL min^{-1} (residence time = 8.4 s).

Effect of residence time. In order to study the effect of the residence time *i.e.* flow rate, the concentration of the precursor and the temperature were kept constant at 2 mM and 200 °C respectively. Residence times were studied between 4.2 and 16.8 s.

Synthesis of CdSe/CdS core/shell nanoparticles

Effect of amount of shelling material. The core CdSe nanoparticles were prepared as mentioned earlier, using a concentration of 2×10^{-2} M of $[Cd(Se_2P^iPr_2)_2]$, at a temperature of 200 °C and under a flow rate of 50 μL min^{-1}. Three different solutions were prepared by mixing $[Cd(S_2CNMe^nHex)_2]$ (1 mg, 2×10^{-3} mmol), (2.5 mg, 5×10^{-3} mmol) and (5 mg, 1×10^{-2} mmol) in OLA (2 mL) each with 4 mL of the as-obtained CdSe nanoparticle solution. The mixed solutions were injected into the microcapillary tube, individually, at 200 °C and under a flow rate of 50 μL min^{-1}; *i.e.* a residence time of 8.4 s. A control reaction was carried out by re-injecting the as-obtained CdSe nanoparticles into the microcapillary reactor under the exact same conditions without adding any CdS precursor.

Effect of shelling residence time. The shelling of the CdSe nanoparticles with CdS shell was carried out at different

residence times by varying the flow rate. The flow rate was varied from 50 to 100 μL min^{-1}; resulting in a residence time from 8.4 s to 4.2 s. All reactions were done by mixing $[Cd(S_2CNMe^nHex)_2]$ (5 mg, 1×10^{-2} mmol) in OLA (2 mL) with 4 mL of the crude CdSe nanoparticles and injecting the mixture into the micro-capillary tube at 200 °C.

Effect of shelling temperature. $[Cd(S_2CNMe^nHex)_2]$ (5 mg, 1×10^{-2} mmol) in OLA (2 mL) was mixed with 4 mL of the crude CdSe nanoparticles and injected into the microcapillary which was pre-heated at 160, 180 or 200 °C under a constant flow rate of 50 μL min^{-1} (residence time = 8.4 s).

Synthesis of alloyed CdSeS nanoparticles

Three different solutions were prepared by adding three different amounts of $[Cd(S_2CNMe^nHex)_2]$ (5×10^{-3} mmol, 2×10^{-2} mmol and 4×10^{-2} mmol) to a fixed concentration of $[Cd(Se_2P^iPr_2)_2]$ (2×10^{-2} M) in TOP (2 mL) followed by addition of 8 mL of OLA in each solution. The solutions were loaded into a syringe and injected into the microcapillary reactor at a flow rate between 12.5 μL min^{-1} and 100 μL min^{-1} (residence time between 33.6 s and 4.2 s, respectively).

Characterization of nanoparticles

X-Ray diffraction studies were performed on a Bruker AXS D8 diffractometer using Cu-Kα radiation. The samples were mounted flat and scanned between 10 and 80° in a step size of 0.05 with a count rate of 9 s. Transmission electron microscopy (TEM), high resolution (HR)TEM and selected area electron diffraction (SAED) analyses were performed using a Tecnai F30 FEG TEM instrument, operating at 300 kV. Nanoparticle samples were simply drop cast onto carbon copper grids. The absorption spectra were recorded on a UV-Vis spectrophotometer (Thermo Spectronic Helios Beta) in the wavelength range of 400–1000 nm. PL measurements of toluene solutions were recorded on a fluoroSENS-fluorimeter. Quantum yields (QYs) were determined by comparison of the integrated fluorescence intensity of nanoparticle dispersion in toluene with that of coumarin solutions in ethanol (QY = 72%) with the optical density (<0.09) at the excitation wavelength (372 nm).

Results and discussion

Cadmium selenide nanoparticles

While CdSe is extensively explored in the traditional batch method, small blue-emitting CdSe nanoparticles remain a challenge.[28] In this work, blue-emitting CdSe nanoparticles were prepared by the thermolysis of the air-stable SSP $[Cd(Se_2P^iPr_2)_2]$ in a microcapillary reactor. A slight blue shift in both the absorption and the emission spectra was observed on increasing the concentration of the precursor (Fig. 2). Increasing the temperature of the oil bath from 180 °C to 200 °C did not cause any significant shift in the band edge of the material, whereas at 220 °C a large red shift was observed due to an increase in the particle size (Fig. 3). The multiply resolved electronic transitions shown in the absorption spectrum of the CdSe nanoparticles grown at 220 °C indicate a narrow size distribution. A red shift

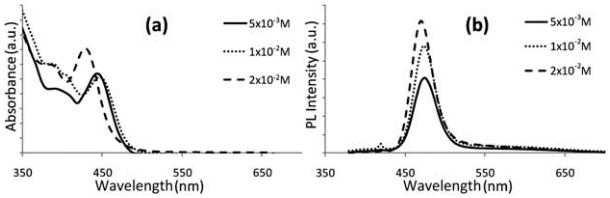

Fig. 2 UV-Vis spectra (a) and PL spectra (b) of CdSe nanoparticles prepared at 200 °C with a residence time of 8.4 s using different concentrations.

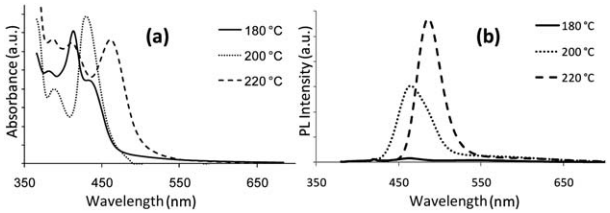

Fig. 3 UV-Vis spectra (a) and PL spectra (b) of CdSe nanoparticles prepared using 2×10^{-2} M solution with a residence time of 8.4 s at different temperatures.

from 464 nm to 470 nm to 480 nm was observed in the emission spectra with the increase in temperature from 180 °C to 200 °C or 220 °C. A red shift in both absorption and emission spectra was also observed when the flow rate was reduced to 25 μL min^{-1} (Fig. 4) to increase the residence time in the reactor and hence allowing the particles to grow bigger.

Calculating the size of the CdSe nanoparticles from their absorption spectra[29] revealed that they are slightly less than 2 nm (1.8 nm to 1.9 nm) except for the samples prepared at the highest temperature (220 °C) or the lowest flow rate (25 μL min^{-1}) which were 2.0 and 2.1 nm, respectively. The band gaps of these CdSe nanoparticles varied between 2.51 eV (494 nm) to 2.73 eV (454 nm) based on their Tauc plots (Fig. 5). The band gap of the bulk CdSe is 1.75 eV. This increase in the band gap is due to the expected quantum confinement effect where the band gap increases as the particle size decreases. The QY ranges from 0.5% to 7% which is similar to the QY obtained in the batch synthesis.[28] In general, an increase in concentration, growth temperature or residence time leads to higher QYs.

CdS nanoparticles

Transmission electron microscopy (TEM). TEM images of the CdS nanoparticles prepared from different concentrations are shown in Fig. 6. Using the lowest concentration of the CdS

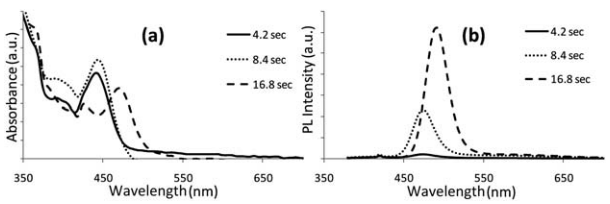

Fig. 4 UV-Vis spectra (a) and PL spectra (b) of CdSe nanoparticles prepared using 2×10^{-2} M solution at 200 °C at different residence times.

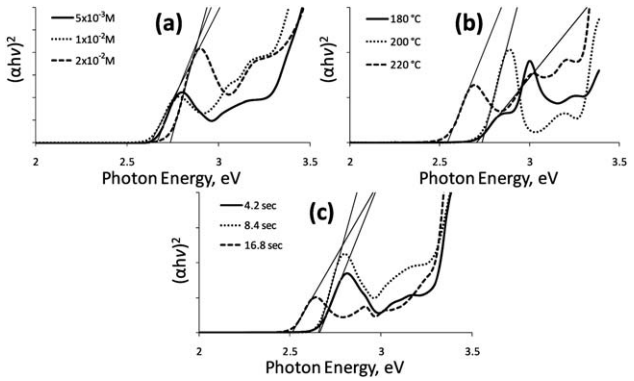

Fig. 5 Tauc plots of the CdSe nanoparticles synthesised at different concentrations (a), different temperatures (b) and different residence times (c).

precursor (0.5 mM) produced aggregated spherical nanoparticles with an average diameter of 5.8 ± 1.5 nm. Increasing the concentration of the precursor to 1 mM resulted in a larger and more monodispersed (7.4 ± 0.9 nm) nanoparticles. On further increasing the concentration to 2 mM, no appreciable change in size was seen.

Optical properties. The UV-Vis spectra and the Tauc plots of OLA capped CdS nanoparticles prepared at various concentrations, temperatures and residence times are shown in Fig. 7, 8 and 9, respectively. A red shift was accompanied with the increase in the concentration, temperature or the residence time, indicating the formation of particles of larger size. The direct band gaps of these CdS nanoparticles range from 2.47 eV (502 nm) to 2.57 eV (482 nm) as calculated from their Tauc plots. Compared to the band gap of the bulk CdS (2.42 eV) there is a slight blue shift between 0.05 eV and 0.15 eV.

CdSe/CdS core/shell nanoparticles

X-Ray diffraction analysis. PXRD patterns of CdSe and CdSe/CdS core/shell nanoparticles are shown in Fig. 10. The core pattern corresponds to cubic CdSe (ICDD card no. 19-0191).

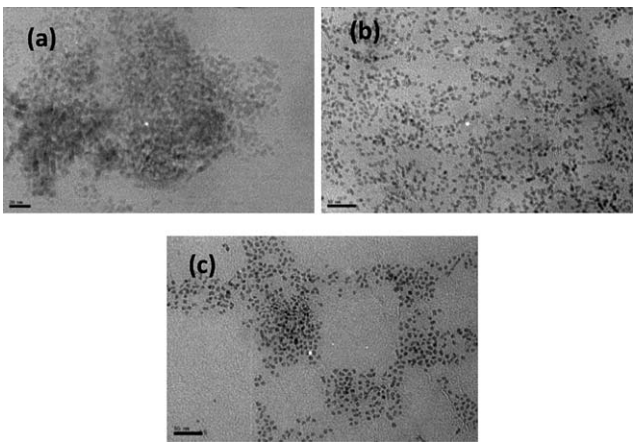

Fig. 6 TEM images of CdS nanoparticles prepared at 200 °C with a residence time of 8.4 s from different precursor concentrations: (a) 0.5 mM, (b) 1 mM and (c) 2 mM. All scale bars are 50 nm.

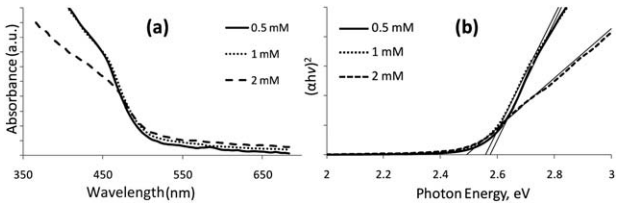

Fig. 7 UV-Vis spectra of CdS nanoparticles prepared at 200 °C with a residence time of 8.4 s from different precursor concentrations (a) and their corresponding Tauc plots (b).

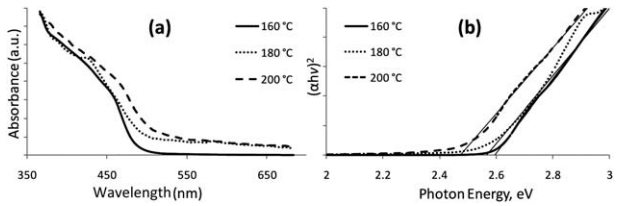

Fig. 8 UV-Vis spectra of CdS nanoparticles prepared using 2 mM solution with a residence time of 8.4 s at different temperatures (a) and their corresponding Tauc plots (b).

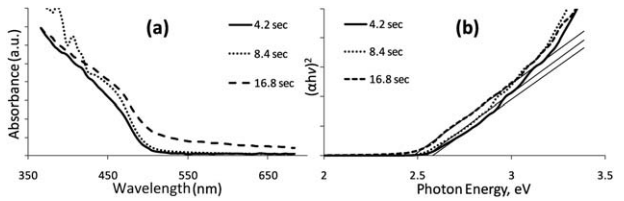

Fig. 9 UV-Vis spectra of CdS nanoparticles prepared using 2 mM solution at 200 °C at different residence times (a) and their corresponding Tauc plots (b).

However, the broad peaks which confirm the small size of the nanoparticles make the distinction between the cubic and hexagonal phases complicated.[30] The core/shell nanoparticles

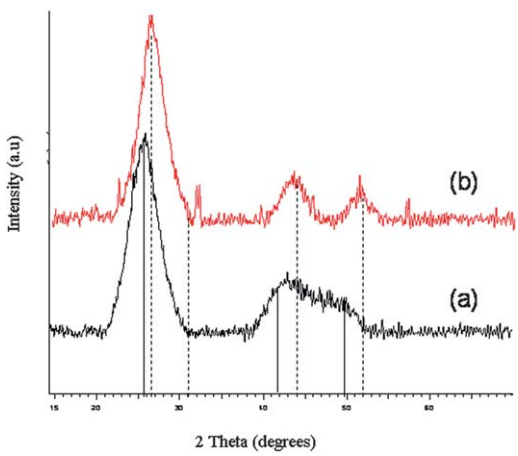

Fig. 10 PXRD pattern of CdSe nanoparticles prepared using 2×10^{-2} M solution at 200 °C and residence time of 8.4 s (a) and CdSe/CdS core/shell nanoparticles prepared using 1×10^{-2} mmol of $[Cd(S_2CNMe^nHex)_2]$ at 200 °C and residence time of 8.4 s (b). Solid and dotted lines represent CdSe and CdS XRD patterns, respectively.

give relatively sharper peaks than that of core. Also the peaks in the PXRD pattern of the CdSe/CdS nanoparticles are slightly shifted to higher angles, towards the position of CdS suggesting that the shell growth is epitaxial, as the lattice mismatch between CdSe and CdS is only 3.9%.[25]

Transmission electron microscopy (TEM). The size of the CdSe and CdSe/CdS core/shell nanoparticles measured from their TEM images (Fig. 11(a) and (b)) is 2.1 ± 0.4 nm and 4.2 ± 0.7 nm, respectively. Since a single monolayer (ML) of CdS shell increases the diameter of the nanoparticles by 0.7 nm,[31] then about 3 MLs have been deposited on top of the core CdSe nanoparticles. The clear lattice planes in the HRTEM images confirm the crystalline nature of the dots. The 3.48 Å lattice spacing in CdSe nanoparticles corresponds to the (111) plane of the bulk cubic crystals consistent with the PXRD data. Energy-dispersive X-ray analysis (EDAX) of the core/shell nanoparticles confirmed the presence of cadmium, selenium and sulfur.

Optical properties. Fig. 12(a) shows the absorption spectra of the core CdSe and the CdSe/CdS core/shell. A clear difference in the absorption band edge is observed. The core/shell nanoparticles show a red shift of ~45 nm (538 nm, 2.30 eV) as compared to the CdSe band edge (492 nm, 2.52 eV). Fig. 12(b) shows enhanced PL intensity as well as a red shift (52 nm) for the core/shell nanoparticles. The QY increased from 7% for the core CdSe to 14% for the CdSe/CdS. The increased QY of the core/shell nanoparticles can be attributed to the elimination of the surface defects/traps and the confinement of the photogenerated exciton in the core due to shelling which is obvious from its symmetrical PL peak. It is worth noting that there was no significant change in the UV-Vis or PL peak observed upon the re-injection of the crude CdSe nanoparticles alone into the microcapillary tube, indicating that the shift observed on injecting a mixture of the as-obtained CdSe nanoparticles and $[Cd(S_2CNMe^nHex)_2]$ is due to the shelling of the CdSe core with a shell of CdS. Moreover, the formation of a core/shell structure and not an alloy is confirmed by the red shift in the absorption and emission spectra. In batch synthesis, most of the reported CdSe/CdS core/shell nanoparticles exhibit an emission peak above 550 nm.[31,32]

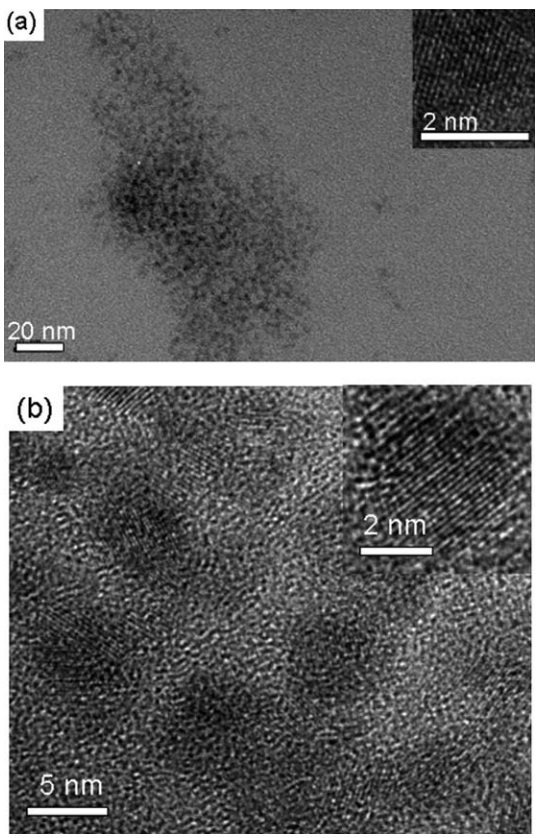

Fig. 11 TEM and HRTEM (insets) images of CdSe nanoparticles prepared using 2×10^{-2} M solution at 200 °C and residence time of 8.4 s (a) and CdSe/CdS core/shell nanoparticles prepared using 1×10^{-2} mmol of $[Cd(S_2CNMe^nHex)_2]$ at 200 °C and residence time of 8.4 s (b).

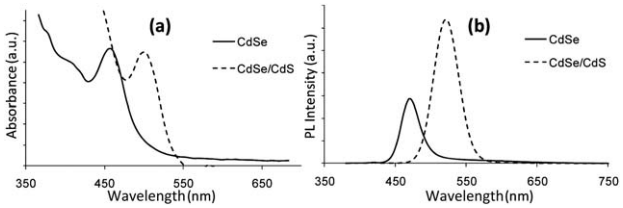

Fig. 12 UV-Vis spectra (a) and PL spectra (b) of the core CdSe nanoparticles prepared using 2×10^{-2} M solution at 200 °C and residence time of 8.4 s and CdSe/CdS core/shell nanoparticles prepared using 1×10^{-2} mmol of $[Cd(S_2CNMe^nHex)_2]$ at 200 °C and residence time of 8.4 s.

Effect of amount of shelling material. To study the effect of the amount of the CdS precursor, three different concentrations of $[Cd(S_2CNMe^nHex)_2]$ were investigated. From the absorption and emission spectra (Fig. 13) it is clear that as more CdS precursor is added, as more red shift is observed, indicating a thicker shell is formed. According to the TEM images (Fig. 14), the average shell thickness was 0.7 ± 0.04 nm (2 MLs) for the (1 mg, 2×10^{-3} mmol), 0.95 ± 0.05 nm (~2.7 MLs) for the (2.5 mg, 5×10^{-3} mmol) and 1.05 ± 0.06 nm (3 MLs) for the (5 mg, 1×10^{-2} mmol) of $[Cd(S_2CNMe^nHex)_2]$. The slight broadening in the size distribution with the growth of the CdS shell is consistent with a previous report.[32] The QYs were 13%, 20% and 14%, for 2 MLs, 2.7 MLs and 3 MLs, respectively, which agree with the previously reported results. In another report,[25] the maximum QY is reported between 2 and 3 monolayers of CdS on CdSe.

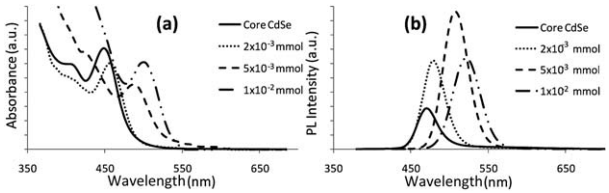

Fig. 13 UV-Vis spectra (a) and PL spectra (b) of the core CdSe nanoparticles prepared using 2×10^{-2} M solution at 200 °C and residence time of 8.4 s and the CdSe/CdS core/shell nanoparticles prepared at 200 °C and residence time of 8.4 s using different concentrations of $[Cd(S_2CNMe^nHex)_2]$.

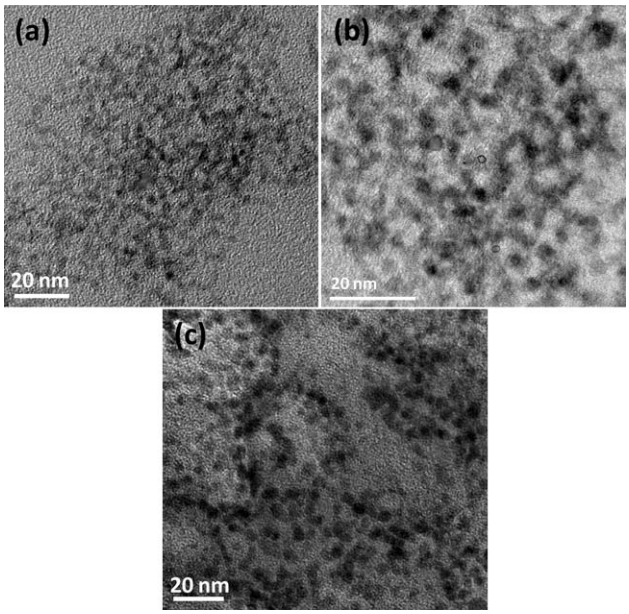

Fig. 14 TEM images of CdSe/CdS core/shell prepared at 200 °C and residence time of 8.4 s with a shell thickness of 2 MLs (a), 2.7 MLs (b) and 3 MLs (c).

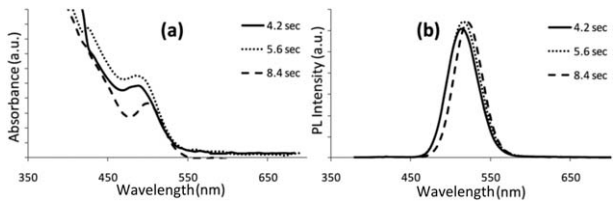

Fig. 15 UV-Vis spectra (a) and PL spectra (b) of the CdSe/CdS core/shell prepared using 1×10^{-2} mmol of $[Cd(S_2CNMe^nHex)_2]$ at 200 °C and at different shelling residence times.

Effect of shelling residence time. Shorter residence times lead to a very small blue shift in both absorption and emission spectra as shown in Fig. 15 for sample prepared using 1×10^{-2} mmol of $[Cd(S_2CNMe^nHex)_2]$ for the shelling step. Similarly, no significant change in the PL intensity was observed.

Effect of shelling temperature. The choice of the shelling temperature is critical as the growth is highly temperature dependent. It was found that for shelling small CdSe nanoparticles (<2.7 nm) with a CdS shell, temperatures above 200 °C would result in Ostwald ripening of the core CdSe and

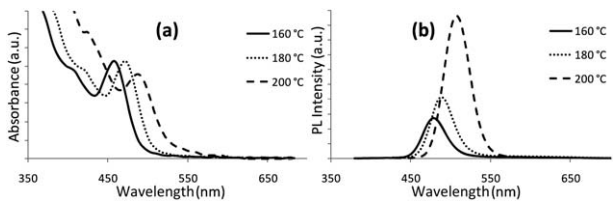

Fig. 16 UV-Vis spectra (a) and PL spectra (b) of the CdSe/CdS core/shell prepared using 1×10^{-2} mmol of $[Cd(S_2CNMe^nHex)_2]$ with a residence time of 8.4 s at different shelling temperatures.

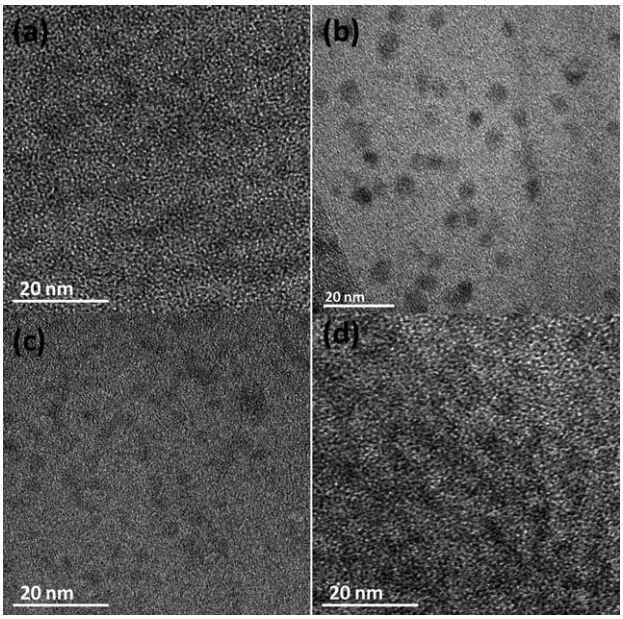

Fig. 17 TEM images of CdSeS nanoparticles prepared using 5×10^{-3} mmol of the CdS precursor at 200 °C at 4.2 s (a), 8.4 s (b), 16.8 s (c) and 33.6 s (d).

defocusing of the size distribution, whereas shelling temperatures far below 200 °C lead to a large amount of the CdS precursor remaining unreacted in the solution with no deposition of the CdS on top of the CdSe; instead homogeneous nucleation of CdS nanoparticles may take place.[15,31,33] In our results, shelling the CdSe nanoparticles with CdS at 160 °C did not show any significant effect on the absorption or emission spectra compared to those of the core CdSe nanoparticles (Fig. 16). Increasing the shelling temperature to 180 °C led to a red shift in both absorption and emission spectra. In terms of QY, a shelling temperature of 200 °C is the most effective (14%).

CdSeS alloy

CdSeS alloys were formed by mixing the CdS precursor $[Cd(S_2CNMe^nHex)_2]$ (5×10^{-3} mmol, 2×10^{-2} mmol and 4×10^{-2} mmol) with a fixed amount of the CdSe precursor $[Cd(Se_2P^iPr_2)_2]$ in TOP/OLA. TEM images of the CdSeS alloys (Fig. 17) prepared using 5×10^{-3} mmol of the CdS precursor at different flow rates revealed that a residence time of 8.4 s or 16.8 s

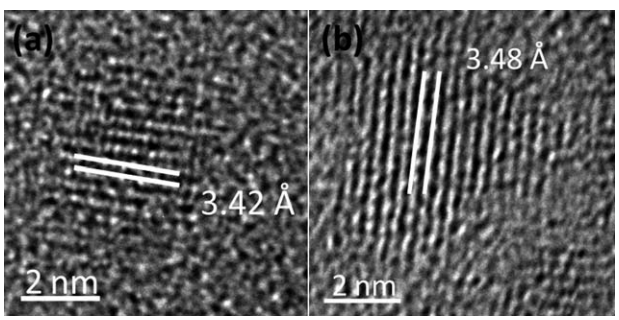

Fig. 18 HRTEM images of CdSeS nanoparticles prepared using 5×10^{-3} mmol of the CdS precursor at 200 °C at (a) 8.4 s and (b) 16.8 s.

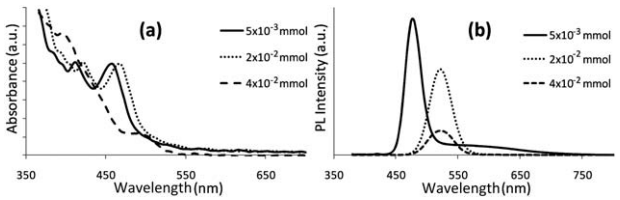

Fig. 19 UV-Vis spectra (a) and PL spectra (b) of CdSeS alloy nanoparticles prepared at 200 °C with a residence time of 8.4 s and using different amounts of $[Cd(S_2CNMe^nHex)_2]$.

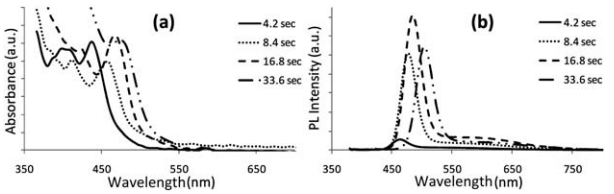

Fig. 20 UV-Vis spectra (a) and PL spectra (b) of the CdSeS alloy nanoparticles prepared using 5×10^{-3} mmol of $[Cd(S_2CNMe^nHex)_2]$, at 200 °C and different residence times.

produced the most monodispersed nanoparticles. The crystalline nature of the CdSeS nanoparticles can be indicated by the clear lattice fringes observed in the HRTEM images (Fig. 18). The *d*-spacing calculated from the HRTEM images of the samples prepared at a residence time of 8.4 s and 16.8 s was 3.42 Å and 3.48 Å, respectively.

Optical properties. Increasing the amount of the CdS precursor resulted in a red shift (Fig. 19) which is probably due to

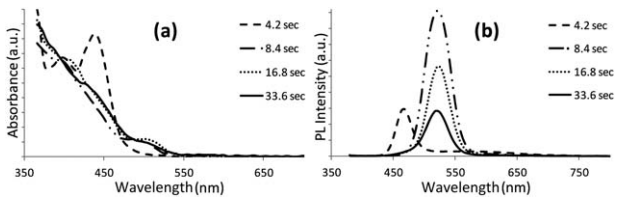

Fig. 21 UV-Vis spectra (a) and PL spectra (b) of the CdSeS alloy nanoparticles prepared using 4×10^{-2} mmol of $[Cd(S_2CNMe^nHex)_2]$, at 200 °C and different residence times.

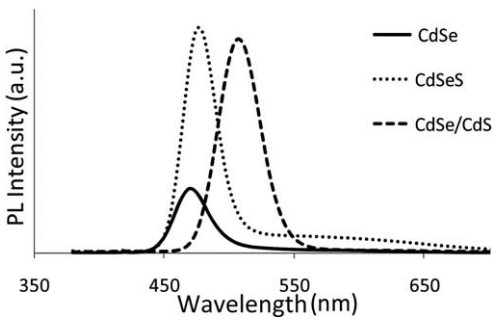

Fig. 22 PL spectra of CdSe nanoparticles prepared using 2×10^{-2} M solution at 200 °C and residence time of 8.4 s, CdSeS alloy and CdSe/CdS core/shell nanoparticles both prepared using the same ratio of CdSe to CdS precursors at 200 °C and residence time of 8.4 s.

increasing the size of the formed nanoparticles. Increasing the amount of the CdS precursor removed the surface traps created by the dangling bonds at the nanoparticles surface, but produced a broader and less intense emission peak. Changing the residence time had an obvious effect with the lowest amount of the CdS precursor (5×10^{-3} mmol). Both absorption and emission spectra showed a continuous red shift with an increase in residence time (Fig. 20). On the other hand, using the highest amount of the CdS precursor (4×10^{-2} mmol), a red shift was only observed by increasing the residence time from 4.2 s to 8.4 s (Fig. 21). Further increase in the residence time (16.8 s or 33.6 s) did not cause any more red shift and resulted in a less intense emission peak. In terms of QY, the lowest amount of the CdS precursor produced the highest QY (13–15%) at residence time between 8.4 s and 33.6 s.

Comparing the average size and the emission position of the CdSe/CdS core/shell (4.0 ± 0.6 nm emitting at 508 nm) and CdSeS alloy (5.0 ± 0.8 emitting at 476 nm), both prepared using 5×10^{-3} mmol of the CdS precursor, shows the formation of CdSeS alloy. Although the alloy is larger in size, its emission peak is blue shifted because of the incorporation of the sulfur (Fig. 22).

Conclusions

Syntheses of CdSe, CdS, CdSe/CdS core/shell, and CdSeS alloy nanoparticles in microcapillary tubes using SSPs have been carried out. Blue emitting, OLA capped CdSe nanoparticles were synthesised from $[Cd(Se_2P^iPr_2)_2]$. Dithiocarbamate $[Cd(S_2CNMe^nHex)_2]$ was shown to be a good candidate for the synthesis of CdS nanoparticles or CdS shell on top of CdSe nanoparticles. CdSeS alloys were synthesised by mixing the two precursors in OLA. Compared to the conventional batch synthesis, continuous synthesis in microreactors provides an efficient and satisfactory route for the synthesis of small bluish-luminescent nanoparticles with good control over size distribution.

Acknowledgements

A.L.A. gratefully acknowledges financial support from the Egyptian Cultural Affairs and Missions Sector. The authors also thank EPSRC, UK for the grants to POB that have made this research possible. P.O.B. wrote this manuscript while a Visiting Fellow at IAS University of Durham. He would like to thank the University for the Fellowship and Collingwood College and its fellows for being gracious hosts.

Notes and references

1 Y. Song, J. Hormes and C. S. S. R. Kumar, *Small*, 2008, **4**, 698.
2 E. M. Chan, R. A. Mathies and A. P. Alivisatos, *Nano Lett.*, 2003, **3**, 199.
3 H. Nakamura, Y. Yamaguchi, M. Miyazaki, H. Maeda, M. Uehara and P. Mulvaney, *Chem. Commun.*, 2002, 2844.
4 H. Nakamura, A. Tashiro, Y. Yamaguchi, M. Miyazaki, T. Watari, H. Shimizu and H. Maeda, *Lab Chip*, 2004, **4**, 237.
5 S. Krishnadasan, J. Tovilla, R. Vilar, A. J. deMello and J. C. deMello, *J. Mater. Chem.*, 2004, **14**, 2655.
6 B. K. H. Yen, N. E. Stott, K. F. Jensen and M. G. Bawendi, *Adv. Mater.*, 2003, **15**, 1858.

7 E. M. Chan, A. P. Alivisatos and R. A. Mathies, *J. Am. Chem. Soc.*, 2005, **127**, 13854.
8 B. K. H. Yen, A. Günther, M. A. Schmidt, K. F. Jensen and M. G. Bawendi, *Angew. Chem., Int. Ed.*, 2005, **44**, 5447.
9 H. Yang, W. Luan, S.-T. Tu and Z. M. Wang, *Lab Chip*, 2008, **8**, 451.
10 H. Yang, W. Luan, S.-T. Tu and Z. M. Wang, *Cryst. Growth Des.*, 2009, **9**, 1569.
11 A. Toyota, H. Nakamura, H. Ozono, K. Yamashita, M. Uehara and H. Maeda, *J. Phys. Chem. C*, 2010, **114**, 7527.
12 B. H. Fischer and M. Giersig, *Langmuir*, 1992, **8**, 1475.
13 J. B. Edel, R. Fortt, J. C. deMello and A. J. deMello, *Chem. Commun.*, 2002, 1136.
14 H. Yang, W. Luan, Z. Wan, S.-T. Tu, W.-K. Yuan and Z. M. Wang, *Cryst. Growth Des.*, 2009, **9**, 4807.
15 J. van Embden, J. Jasieniak, D. E. Gomez, P. Mulvaney and M. Giersig, *Aust. J. Chem.*, 2007, **60**, 457.
16 H. Wang, X. Li, M. Uehara, Y. Yamaguchi, H. Nakamura, M. Miyazaki, H. Shimizu and H. Maeda, *Chem. Commun.*, 2004, 48.
17 H. Wang, H. Nakamura, M. Uehara, Y. Yamaguchi, M. Miyazaki and H. Maeda, *Adv. Funct. Mater.*, 2005, **15**, 603.
18 W. Luan, H. Yang, N. Fan and S.-T. Tu, *Nanoscale Res. Lett.*, 2008, **3**, 134.
19 M. D. Regulacio and M.-Y. Han, *Acc. Chem. Res.*, 2010, **43**, 621.
20 L. A. Swafford, L. A. Weigand, M. J. Bowers, J. R. McBride, J. L. Rapaport, T. L. Watt, S. K. Dixit, L. C. Feldman and S. J. Rosenthal, *J. Am. Chem. Soc.*, 2006, **128**, 12299.
21 N. Al-Salim, A. G. Young, R. D. Tilley, A. J. McQuillan and J. Xia, *Chem. Mater.*, 2007, **19**, 5185.
22 J. Ouyang, M. Vincent, D. Kingston, P. Descours, T. Boivineau, Md. B. Zaman, X. Wu and K. Yu, *J. Phys. Chem. C*, 2009, **113**, 5193.
23 X. Zhong, Y. Feng and Y. Zhang, *J. Phys. Chem. C*, 2007, **111**, 526.
24 L. Qu and X. Peng, *J. Am. Chem. Soc.*, 2002, **124**, 2049.
25 X. Peng, M. C. Schlamp, A. V. Kadavanich and A. P. Alivisatos, *J. Am. Chem. Soc.*, 1997, **119**, 7019.
26 C. Q. Naguyen, M. Afzaal, M. A. Malik, M. Helliwell, J. Raftery and P. O'Brien, *J. Organomet. Chem.*, 2007, **692**, 2669.
27 M. A. Malik, N. Revaprasadu and P. O'Brien, *Chem. Mater.*, 2001, **13**, 913.
28 R. K. Čapek, K. Lambert, D. Dorfs, P. F. Smet, D. Poelman, A. Eychmüller and Z. Hens, *Chem. Mater.*, 2009, **21**, 1743.
29 W. W. Yu, L. Qu, W. Guo and X. Peng, *Chem. Mater.*, 2003, **15**, 2854.
30 C. B. Murray, D. J. Norris and M. G. Bawendi, *J. Am. Chem. Soc.*, 1993, **115**, 8706.
31 J. J. Li, Y. A. Wang, W. Guo, J. C. Keay, T. D. Mishima, M. B. Johnson and X. Peng, *J. Am. Chem. Soc.*, 2003, **125**, 12567.
32 N. Revaprasadu, M. A. Malik, P. O'Brien and G. Wakefield, *Chem. Commun.*, 1999, 1573.
33 J. van Embden, J. Jasieniak and P. Mulvaney, *J. Am. Chem. Soc.*, 2009, **131**, 14299.